Spin-s Dicke States and Their Preparation

Rafael I. Nepomechie, Francesco Ravanini, and David Raveh*

The notion of $su(2)$ spin-s Dicke states is introduced, which are higher-spin generalizations of usual (spin-1/2) Dicke states. These multi-qudit states can be expressed as superpositions of $su(2s+1)$ qudit Dicke states. They satisfy a recursion formula, which is used to formulate an efficient quantum circuit for their preparation, whose size scales as $sk(2sn-k)$, where n is the number of qudits and k is the number of times the total spin-lowering operator is applied to the highest-weight state. The algorithm is deterministic and does not require ancillary qudits.

1. Introduction

Quantum state preparation is a fundamental task in quantum computing.[1] The cost of preparing a general quantum state scales exponentially with the number of qubits (or qudits, for d-level systems), see e.g. refs. [2–6]. Hence, quantum states that can be prepared efficiently are of particular interest. Dicke states[7] constitute one such example. These states, which we denote here by $|D_{n,k}\rangle$, are completely symmetric n-qubit states of k $|1\rangle$'s and $n-k$ $|0\rangle$'s, for instance

$$|D_{3,2}\rangle = \frac{1}{\sqrt{3}}(|011\rangle + |101\rangle + |110\rangle) \tag{1}$$

where the tensor product is understood, e.g. $|011\rangle = |0\rangle \otimes |1\rangle \otimes |1\rangle$. Such states have numerous applications, including quantum networking,[8] quantum metrology,[9] optimization,[10] and quantum compression.[11] An efficient algorithm for preparing Dicke states was given in ref. [11], see also refs. [12, 13]. This construction was used recently as the starting point for preparing exact eigenstates of the Heisenberg spin chain[14–16] via coordinate Bethe ansatz.[17,18]

A generalization of Dicke states $|D_{n,k}\rangle$ to higher-level systems is given by qudit Dicke states, which are multi-qudit completely symmetric basis states (a precise definition can be found in Appendix A); and an algorithm for preparing these states, generalizing ref. [11],[11] was given in ref. [19].

Additional types of quantum states that can be prepared efficiently include the q-deformation of qubit[20] and qudit[21] Dicke states, uniform and cyclic quantum states,[22] and W states.[23]

In this paper, we introduce the notion of higher-spin Dicke states, and we formulate a deterministic algorithm for preparing these states that does not require ancillas. These multi-qudit states differ from the above-mentioned qudit Dicke states, and can in fact be prepared with significantly simpler circuits. We expect that these states may be useful for generalizing the many applications of (qubit) Dicke states to qudits, and may serve as the starting point for preparing exact eigenstates of integrable higher-spin Heisenberg chains via coordinate Bethe ansatz.[24]

Specifically, we consider qudits with dimension $d = 2s+1$, where $s = 1/2, 1, 3/2, \ldots$, corresponding to spin-s spins. We denote the basis by

$$|0\rangle = \begin{pmatrix}1\\0\\\vdots\\0\end{pmatrix}, |1\rangle = \begin{pmatrix}0\\1\\\vdots\\0\end{pmatrix}, \ldots, |2s\rangle = \begin{pmatrix}0\\0\\\vdots\\1\end{pmatrix} \tag{2}$$

as usual. The total spin operators $\vec{\mathbb{S}}$ are given by

$$\vec{\mathbb{S}} = \sum_{i=0}^{n-1} \vec{\mathbb{S}}_i, \qquad \vec{\mathbb{S}}_i = \overset{n-1}{\overset{\downarrow}{\mathbb{I}}} \otimes \ldots \otimes \mathbb{I} \otimes \overset{i}{\overset{\downarrow}{\vec{S}}} \otimes \mathbb{I} \otimes \ldots \otimes \overset{0}{\overset{\downarrow}{\mathbb{I}}} \tag{3}$$

where $\vec{S} = (S^x, S^y, S^z)$ are $(2s+1)\times(2s+1)$ matrices that obey the $su(2)$ algebra $[S^x, S^y] = iS^z$, etc., and $\mathbb{I}$ is the $(2s+1)\times(2s+1)$ identity matrix. As usual, we take S^z to be the diagonal matrix

$$S^z = \text{diag}\,(s, s-1, \ldots, -(s-1), -s) \tag{4}$$

For a system of n such qudits, we define spin-s Dicke states $|D^{(s)}_{n,k}\rangle$ as the states obtained by applying k times the total spin-lowering operator $\mathbb{S}^-$ on the highest-weight state. More precisely,

$$|D^{(s)}_{n,k}\rangle = a^{(s)}_{n,k}(\mathbb{S}^-)^k|0\rangle^{\otimes n}, \qquad k = 0, 1, \ldots, 2sn \tag{5}$$

R. I. Nepomechie, D. Raveh
Department of Physics
University of Miami
P.O. Box 248046, Coral Gables, FL 33124, USA
E-mail: nepomechie@miami.edu

F. Ravanini
Department of Physics and Astronomy
University of Bologna
Via Irnerio 46, Bologna I-40126, Italy

F. Ravanini
INFN
Sezione di Bologna
Via Irnerio 46, Bologna I-40126, Italy

The ORCID identification number(s) for the author(s) of this article can be found under https://doi.org/10.1002/qute.202400057

DOI: 10.1002/qute.202400057

where $\mathbb{S}^- = \mathbb{S}^x - i\mathbb{S}^y$ is the total spin-lowering operator, $|0\rangle^{\otimes n}$ is the state with all n spins "up" (with $\mathbb{S}^z$-eigenvalue $\mathbb{m} = sn$), and $a^{(s)}_{n,k}$ is the normalization factor (This factor can be derived using the familiar fact

$$\mathbb{S}^- |\mathbb{s}, \mathbb{m}\rangle = \sqrt{(\mathbb{s}+\mathbb{m})(\mathbb{s}+1-\mathbb{m})}\, |\mathbb{s}, \mathbb{m}-1\rangle \tag{6}$$

where $|\mathbb{s}, \mathbb{m}\rangle$ are simultaneous eigenstates of $\vec{\mathbb{S}}^2$ and $\mathbb{S}^z$, and the fact that here $\mathbb{s} = sn$.).

$$a^{(s)}_{n,k} = \frac{1}{k!\sqrt{\binom{2sn}{k}}} \tag{7}$$

These states are exact ground states of ferromagnetic spin-s Heisenberg Hamiltonians, and of a spin-s version of the Lipkin–Meshkov–Glick[25] Hamiltonian $-\vec{\mathbb{S}}^2 = -\sum_{i,j} \vec{S}_i \cdot \vec{S}_j$.

The spin-s Dicke states take the closed-form expression

$$|D^{(s)}_{n,k}\rangle = \sum_{\substack{j_i=0,1,\ldots,2s \\ j_0+j_1+\cdots+j_{n-1}=k}} \sqrt{\frac{\binom{2s}{j_0}\binom{2s}{j_1}\cdots\binom{2s}{j_{n-1}}}{\binom{2sn}{k}}}\, |j_{n-1}\ldots j_1 j_0\rangle \tag{8}$$

see Appendix A for a complete proof of this fact. Thus, for $s = 1/2$ the spin-s Dicke states reduce to the usual Dicke states, i.e. $|D^{(1/2)}_{n,k}\rangle = |D_{n,k}\rangle$. Further, for $s > 1/2$, these states can be expressed as linear combinations of $(2s+1)$-level qudit Dicke states. A simple example with $s = 1$ is the state

$$\begin{aligned} |D^{(1)}_{3,2}\rangle &= \frac{2}{\sqrt{15}}(|011\rangle + |101\rangle + |110\rangle) \\ &\quad + \frac{1}{\sqrt{15}}(|002\rangle + |020\rangle + |200\rangle) \end{aligned} \tag{9}$$

The general relation between higher-spin and qudit Dicke states is given by Equations (A10) and (A13). Higher-spin Dicke states are entangled, and we include here a computation of their bipartite entanglement entropy. We remark that these states have the "duality" (charge conjugation) transformation property

$$C^{\otimes n}\, |D^{(s)}_{n,k}\rangle = |D^{(s)}_{n,2sn-k}\rangle\,, \qquad C = \begin{pmatrix} & & 1 \\ & \iddots & \\ 1 & & \end{pmatrix} \tag{10}$$

which maps $k \mapsto 2sn - k$. To our knowledge, such higher-spin Dicke states have not heretofore been systematically studied.[26,27]

An outline of the reminder of the paper is as follows. In Section 2, we present a recursive construction of higher-spin Dicke states on a quantum computer. (Of course, the construction Equation (5) cannot be directly implemented on a quantum computer, since the total spin-lowering operator $\mathbb{S}^-$ is not unitary.) The key idea is that, as for the case of usual Dicke states[11] and qudit Dicke states,[19,21] these states satisfy a recursion Equation (17), which is proved in Appendix B. The reference state Equation (14), whose choice requires considerable care, also plays an important role in this construction. The problem reduces to finding explicit circuits for certain operators T. As a warm-up for determining these T operators, we briefly review in Section 3 the case $s = 1/2$.[11,19] In Section 4, we consider the case $s = 1$; and we finally treat the general spin-s case in Section 5. We conclude with a brief discussion in Section 6. We complement the paper with some appendices; in particular, Appendix A shows the relation between higher-spin and qudit Dicke states, and Appendix C contains the computation of the entanglement entropy. Code in cirq[28] for simulating the circuits presented here is provided in the Supporting Information.

2. Recursive Construction

We assume that a spin-s Dicke state Equation (5) can be generated by a unitary operator $U^{(s)}_n$ acting on a simple "reference" state $|\psi^{(s)}_{n,k}\rangle$

$$|D^{(s)}_{n,k}\rangle = U^{(s)}_n\, |\psi^{(s)}_{n,k}\rangle\,, \qquad k = 0, 1, \ldots, 2sn \tag{11}$$

where $U^{(s)}_n$ is independent of k.

In order to specify the reference state $|\psi^{(s)}_{n,k}\rangle$ for a given value of k, it is necessary to first define ℓ to be the unique integer satisfying

$$k = 2s\ell + i\,, \qquad 0 \le i < 2s \tag{12}$$

so that

$$\ell = \lfloor \frac{k}{2s} \rfloor \in \{0, 1, \ldots, n\}\,, \quad i = k - 2s\ell \in \{0, 1, \ldots, 2s-1\} \tag{13}$$

where $\lfloor \ldots \rfloor$ denotes floor. The reference state $|\psi^{(s)}_{n,k}\rangle$ is then given by the product state

$$|\psi^{(s)}_{n,k}\rangle \equiv |\psi^{(s)\,i}_{n\,;\ell}\rangle = |0\rangle^{\otimes(n-\ell-1)}|i\rangle|2s\rangle^{\otimes \ell} \tag{14}$$

These reference states have been engineered so that they reduce for $n = 1$ to basis states $|k\rangle$

$$|\psi^{(s)}_{1,k}\rangle = |k\rangle = |D^{(s)}_{1,k}\rangle\,, \qquad k = 0, 1, \ldots, 2s \tag{15}$$

which implies that $U^{(s)}_n$ in Equation (11) reduces for $n = 1$ to the identity matrix

$$U^{(s)}_1 = \mathbb{I} \tag{16}$$

A key feature of spin-s Dicke states Equation (5) is that they obey a recursion formula

$$|D^{(s)}_{n,k}\rangle = \sum_{j=0}^{2s} c^{(s)}_{n,k,j}\, |D^{(s)}_{n-1,k-j}\rangle \otimes |j\rangle \tag{17}$$

with

$$c^{(s)}_{n,k,j} = \sqrt{\frac{\binom{2s}{j}\binom{2sn-2s}{k-j}}{\binom{2sn}{k}}} \tag{18}$$

whose proof is given in Appendix B. Similarly to refs. [11, 19, 21], let us now define a unitary operator $W_n^{(s)}$ that implements a corresponding mapping on the reference states

$$W_n^{(s)}\,|\psi_{n,k}^{(s)}\rangle = \sum_{j=0}^{2s} c_{n,k,j}^{(s)}\,|\psi_{n-1,k-j}^{(s)}\rangle \otimes |j\rangle\,, \qquad n = 2, 3, \ldots \tag{19}$$

Note that $W_n^{(s)}$, like $U_n^{(s)}$, is independent of k. Making use of Equation (11) in both sides of Equation (17), we see that $U_n^{(s)}$ satisfies the recursion

$$U_n^{(s)} = \left(U_{n-1}^{(s)} \otimes \mathbb{I}\right) W_n^{(s)} \tag{20}$$

Telescoping the recursion, and imposing the initial condition Equation (16), we conclude that $U_n^{(s)}$ is given by an ordered product of W operators

$$U_n^{(s)} = \overset{\curvearrowright}{\prod_{m=2}^{n}} \left(W_m^{(s)} \otimes \mathbb{I}^{\otimes(n-m)}\right) \tag{21}$$

where the product goes from left to right with increasing m.

The problem of constructing a quantum circuit for $U_n^{(s)}$ therefore reduces to finding circuits for the $W_m^{(s)}$ operators. The strategy for accomplishing the latter is to look for operators $T_{m,k}^{(s)} \equiv T_{m;\ell}^{(s)\,i}$ (recall the Equations (12) and (13) for ℓ and i), which *do* depend on k, with the following properties

$$T_{m,k'}^{(s)}\,|\psi_{m,k}^{(s)}\rangle = \begin{cases} |\psi_{m,k}^{(s)}\rangle & \text{for} \quad k' < k \qquad (22) \\ W_m^{(s)}\,|\psi_{m,k}^{(s)}\rangle & \text{for} \quad k' = k \qquad (23) \end{cases}$$

and

$$T_{m,k'}^{(s)}\left(T_{m,k}^{(s)}\,|\psi_{m,k}^{(s)}\rangle\right) = \left(T_{m,k}^{(s)}\,|\psi_{m,k}^{(s)}\rangle\right) \quad \text{for} \quad k' > k \tag{24}$$

where $W_m^{(s)}\,|\psi_{n,k}^{(s)}\rangle$ in Equation (23) is given by Equation (19). An operator $W_m^{(s)}$ that performs the mapping Equation (19) is therefore given by an ordered product of all the T operators

$$W_m^{(s)} = \overset{\curvearrowleft}{\prod_{k=1}^{2sm-1}} T_{m,k}^{(s)} \tag{25}$$

where the product goes from right to left with increasing k.

We see from Equation (25) that the number of T operators in $W_m^{(s)}$ is $2sm - 1$; and from Equation (21) we conclude that the number of T operators in $U_n^{(s)}$ is

$$\sum_{m=2}^{n}(2sm-1) = \mathcal{O}(n^2 s) \tag{26}$$

However, we shall later argue that the number of T operators can be reduced, see Equation (52).

To summarize, spin-s Dicke states Equation (5) are generated by Equation (11), where the reference state $|\psi_{n,k}^{(s)}\rangle$ is given by Equation (14), the unitary operator $U_n^{(s)}$ is given in terms of W's by Equation (21), and the W's are given in terms of T's by Equation (25). It remains to find explicit circuits for the T's, to which the reminder of this paper is largely dedicated. As a warm-up, we begin by reviewing the case $s = 1/2$ in Section 3; we then treat the case $s = 1$ in Section 4, and we finally consider the general spin-s case in Section 5.

3. The Case $s = 1/2$

For the case $s = 1/2$, which corresponds to usual qubit Dicke states, we see from Equation (12) that $\ell = k$ and $i = 0$; hence, the reference state Equation (14) with $n = m$ reduces to

$$|\psi_{m,k}^{(1/2)}\rangle = |0\rangle^{\otimes(m-k)}|1\rangle^{\otimes k} \tag{27}$$

The action of the W operator on this state is given by Equation (19)

$$\begin{aligned} W_m^{(1/2)}\,|0\rangle^{\otimes(m-k)}|1\rangle^{\otimes k} &= c_{m,k,0}^{(1/2)}\,|0\rangle^{\otimes(m-k-1)}|1\rangle^{\otimes k}|0\rangle \\ &+ c_{m,k,1}^{(1/2)}\,|0\rangle^{\otimes(m-k)}|1\rangle^{\otimes k} \end{aligned} \tag{28}$$

We define a three-qubit operator $T_{m,k}^{(1/2)}$ (denoted by $\mathrm{I}_{m,k}$ in refs. [19, 21]) that performs the mapping Equation (23) with Equation (28), which acts on the kth, $(k-1)$th, and 0th qubit, as follows

$$\begin{aligned} T_{m,k}^{(1/2)}: \quad |0\rangle_k\,|1\rangle_{k-1}\,|1\rangle_0 \;\mapsto\; & c_{m,k,0}^{(1/2)}\,|1\rangle_k\,|1\rangle_{k-1}\,|0\rangle_0 \\ &+ c_{m,k,1}^{(1/2)}\,|0\rangle_k\,|1\rangle_{k-1}\,|1\rangle_0 \end{aligned} \tag{29}$$

and otherwise acts as identity (as long as the 0th qubit is in the state $|1\rangle$, which is always the case for the input states in Equation (28)). For $k = 1$, the middle qubits in Equation (29) are omitted. The corresponding circuit diagrams are shown in **Figure 1**, where here $R(\theta)$ is the $R^y(-\theta)$-gate

$$R(\theta) = \begin{pmatrix} \cos(\theta/2) & \sin(\theta/2) \\ -\sin(\theta/2) & \cos(\theta/2) \end{pmatrix} \tag{30}$$

and the angle θ_1 is chosen such that

$$\cos(\theta_1/2) = c_{m,k,1}^{(1/2)} \tag{31}$$

Throughout the paper, we label m-qudit vector spaces from 0 to $m-1$, going from right to left, as in Equation (3); and in circuit diagrams, the m vector spaces are represented by corresponding wires labeled from the top (0) to the bottom $(m-1)$.

3.1. Simplifying the Circuit

We have seen that the operator $U_n^{(1/2)}$ is given by Equations (21), (25), and (29). According to Equation (11), this operator generates the Dicke states $|D_{n,k}\rangle$ for *all* possible values of k. However, if we are only interested in a Dicke state for a *fixed* value of k, then it can be shown that some of the T operators become redundant;

(a) $T^{(1/2)}_{m,k}$ with $k > 1$ (b) $T^{(1/2)}_{m,k}$ with $k = 1$

Figure 1. Circuit diagrams for $T^{(1/2)}_{m,k}$.

by removing those redundant operators, we are left with a "simplified" k-dependent operator $\mathcal{U}^{(1/2)}_{n,k}$ that creates the desired state

$$|D_{n,k}\rangle = \mathcal{U}^{(1/2)}_{n,k}\, |\psi^{(1/2)}_{n,k}\rangle \tag{32}$$

This simplified operator is expressed similarly to Equation (21) in terms of corresponding simplified operators $\mathcal{W}^{(1/2)}_{m,k}$

$$\mathcal{U}^{(1/2)}_{n,k} = \prod_{m=2}^{\overset{\curvearrowright}{n}} \left(\mathcal{W}^{(1/2)}_{m,k} \otimes \mathbb{I}^{\otimes(n-m)} \right) \tag{33}$$

where[19,21]

$$\mathcal{W}^{(1/2)}_{m,k} = \prod_{k'=\max(k+m-n,1)}^{\overset{\curvearrowleft}{\min(k,m-1)}} T^{(1/2)}_{m,k'} \tag{34}$$

cf. Equation (25).

4. The Case $s = 1$

We turn now to the construction of the spin-1 T operators. For $s = 1$, we see from (12) that i can have two possible values: either $i = 0$ (k is even and $\ell = k/2$), or $i = 1$ (k is odd and $\ell = (k-1)/2$). Correspondingly, there are two families of reference states

$$|\psi^{(1)\,0}_{m;\ell}\rangle = |0\rangle^{\otimes(m-\ell)}|2\rangle^{\otimes\ell} ,$$
$$|\psi^{(1)\,1}_{m;\ell}\rangle = |0\rangle^{\otimes(m-\ell-1)}|1\rangle|2\rangle^{\otimes\ell} \tag{35}$$

where the subscripted semicolon notation is defined in Equation (14). The action of the W operator on these reference states is given, according to Equation (19), by

$$\begin{aligned} W^{(1)}_m\, |0\rangle^{\otimes(m-\ell)}|2\rangle^{\otimes\ell} &= c^{(1)}_{m,k,0}\, |0\rangle^{\otimes(m-\ell-1)}|2\rangle^{\otimes\ell}|0\rangle \\ &+ c^{(1)}_{m,k,1}\, |0\rangle^{\otimes(m-\ell-1)}|1\rangle|2\rangle^{\otimes(\ell-1)}|1\rangle \\ &+ c^{(1)}_{m,k,2}\, |0\rangle^{\otimes(m-\ell)}|2\rangle^{\otimes\ell} , \qquad k = 2\ell \end{aligned} \tag{36}$$

$$\begin{aligned} W^{(1)}_m\, |0\rangle^{\otimes(m-\ell-1)}|1\rangle|2\rangle^{\otimes\ell} &= c^{(1)}_{m,k,0}\, |0\rangle^{\otimes(m-\ell-2)}|1\rangle|2\rangle^{\otimes\ell}|0\rangle \\ &+ c^{(1)}_{m,k,1}\, |0\rangle^{\otimes(m-\ell-1)}|2\rangle^{\otimes\ell}|1\rangle \\ &+ c^{(1)}_{m,k,2}\, |0\rangle^{\otimes(m-\ell-1)}|1\rangle|2\rangle^{\otimes\ell} , k = 2\ell+1 \end{aligned} \tag{37}$$

respectively. We will treat these two cases separately in turn, see Equations (39) and (41) below.

In order to implement these operators, we make use of the ternary quantum logic gates defined in ref. [29] (see also ref. [30]). In particular, we denote by $X^{(i,j)}$, with $i < j$, the NOT gate that performs the interchange $|i\rangle \leftrightarrow |j\rangle$ and leaves unchanged the remaining basis vector. Similarly, $R^{(i,j)}(\theta)$ denotes the gate that performs an $R^y(-\theta)$ rotation in the subspace spanned by $|i\rangle$ and $|j\rangle$; hence,

$$R^{(i,j)}(\theta)|i\rangle = \cos(\theta/2)|i\rangle - \sin(\theta/2)|j\rangle ,$$
$$R^{(i,j)}(\theta)|j\rangle = \sin(\theta/2)|i\rangle + \cos(\theta/2)|j\rangle \tag{38}$$

Moreover, $\textcircled{i}$ denotes a control (of a controlled gate) with value i.

For k even, we define the three-qutrit operator $T^{(1)}_{m,k} = T^{(1)}_{m,2\ell} \equiv T^{(1)\,0}_{m;\ell}$ that performs the mapping Equation (23) with Equation (36) as follows

$$\begin{aligned} T^{(1)\,0}_{m;\ell} : \quad & |0\rangle_\ell\, |2\rangle_{\ell-1}\, |2\rangle_0 \mapsto c^{(1)}_{m,k,0}\, |2\rangle_\ell\, |2\rangle_{\ell-1}\, |0\rangle_0 \\ & + c^{(1)}_{m,k,1}\, |1\rangle_\ell\, |2\rangle_{\ell-1}\, |1\rangle_0 + c^{(1)}_{m,k,2}\, |0\rangle_\ell\, |2\rangle_{\ell-1}\, |2\rangle_0 , \quad k = 2\ell \end{aligned} \tag{39}$$

and otherwise acts as identity (as long as the 0th qutrit is in the state $|2\rangle$, which is always the case for the input states in Equation (36)). For $\ell = 1$, the middle qutrits in Equation (39) are omitted. The corresponding circuit diagram (with $1 < \ell \leq m-1$ and $m > 2$) is given in **Figure 2**, where the rotation angles θ_1 and θ_2 are chosen such that

$$\cos(\theta_1/2) = c^{(1)}_{m,k,2} , \qquad \sin(\theta_1/2)\cos(\theta_2/2) = c^{(1)}_{m,k,1} ,$$
$$\sin(\theta_1/2)\sin(\theta_2/2) = c^{(1)}_{m,k,0} \tag{40}$$

The circuit for the edge cases with $l = 1$ and $m > 1$ can be obtained as a limit of the circuit in Figure 2, see Appendix D.

For k odd, we similarly define a four-qutrit operator $T^{(1)}_{m,k} = T^{(1)}_{m,2\ell+1} \equiv T^{(1)\,1}_{m;\ell}$ that performs the mapping Equation (23) with

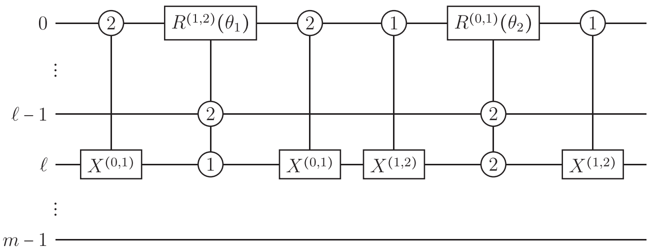

Figure 2. Circuit diagram for $T^{(1)}_{m,k} = T^{(1)}_{m,2\ell} = T^{(1)\,0}_{m;\ell}$ (k even), with $1 < \ell \leq m-1$, $m > 2$.

Equation (37) as follows

$$
\begin{aligned}
T^{(1)\,1}_{m;\ell}: \quad & |0\rangle_{\ell+1}\,|1\rangle_{\ell}\,|2\rangle_{\ell-1}\,|2\rangle_0 \mapsto c^{(1)}_{m,k,0}\,|1\rangle_{\ell+1}\,|2\rangle_{\ell}\,|2\rangle_{\ell-1}\,|0\rangle_0 \\
& + c^{(1)}_{m,k,1}\,|0\rangle_{\ell+1}\,|2\rangle_{\ell}\,|2\rangle_{\ell-1}\,|1\rangle_0 \\
& + c^{(1)}_{m,k,2}\,|0\rangle_{\ell+1}\,|1\rangle_{\ell}\,|2\rangle_{\ell-1}\,|2\rangle_0\,, k = 2\ell+1
\end{aligned} \tag{41}
$$

The corresponding circuit diagram (with $1 < \ell < m-1$ and $m > 3$) is given in **Figure** 3, where the rotation angles θ_1 and θ_2 are again given by Equation (40).

For the four types of edge cases for $T^{(1)\,1}_{m;\ell}$

1) $\ell = m-1\,,\, m > 2$
2) $\ell = 1\,,\, m = 2$
3) $\ell = 1\,,\, m > 3$
4) $\ell = 0\,,\, m > 1$

the corresponding circuit diagrams can be obtained from limits of Figure 3, see Appendix D.

One can check that the T operators defined by these circuits indeed also satisfy the property Equation (24). Code in cirq[28] for simulating these circuits is included in the Supporting Information.

4.1. Simplifying the Circuit

As discussed for the case $s = 1/2$ in Section 3.1, for a fixed value of k, not all T operators are needed; by removing the redundant operators, we are left with a "simplified" k-dependent operator $\mathcal{U}^{(1)}_{n,k}$ that generates the desired state

$$
|D^{(1)}_{n,k}\rangle = \mathcal{U}^{(1)}_{n,k}\,|\psi^{(1)}_{n,k}\rangle \tag{42}
$$

where

$$
\mathcal{U}^{(1)}_{n,k} = \overset{\curvearrowright}{\prod_{m=2}^{n}} \left(\mathcal{W}^{(1)}_{m,k} \otimes \mathbb{I}^{\otimes(n-m)} \right) \tag{43}
$$

and

$$
\mathcal{W}^{(1)}_{m,k} = \overset{\curvearrowleft}{\prod_{k'=\max(k+2(m-n),1)}^{\min(k,2m-1)}} T^{(1)}_{m,k'} \tag{44}
$$

5. The Spin-*s* Case

We now turn to the construction of the T operators for general values of spin. For spin s, there are $2s$ possible values of i in Equation (12). We observe from Equations (19) and (23) that

$$
T^{(s)\,i}_{m;\ell}\,|\psi^{(s)\,i}_{m;\ell}\rangle = \sum_{j=0}^{2s} c^{(s)}_{m,2s\ell+i,j}\,|\psi^{(s)}_{m-1,2s\ell+i-j}\rangle \otimes |j\rangle \tag{45}
$$

Recalling that the reference states are given by Equation (14), and noting that

$$
|\psi^{(s)}_{m-1,2s\ell+i-j}\rangle = \begin{cases} |\psi^{(s)\,i-j}_{m-1;\ell}\rangle & i \geq j \\ |\psi^{(s)\,2s+i-j}_{m-1;\ell-1}\rangle & i < j \end{cases} \tag{46}
$$

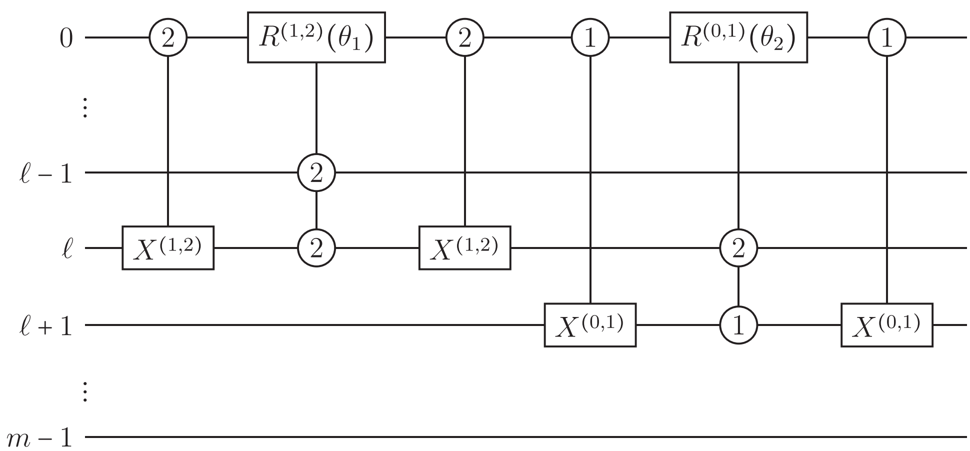

Figure 3. Circuit diagram for $T^{(1)}_{m,k} = T^{(1)}_{m,2\ell+1} = T^{(1)\,1}_{m;\ell}$ (k odd), with $1 < \ell < m-1$, $m > 3$.

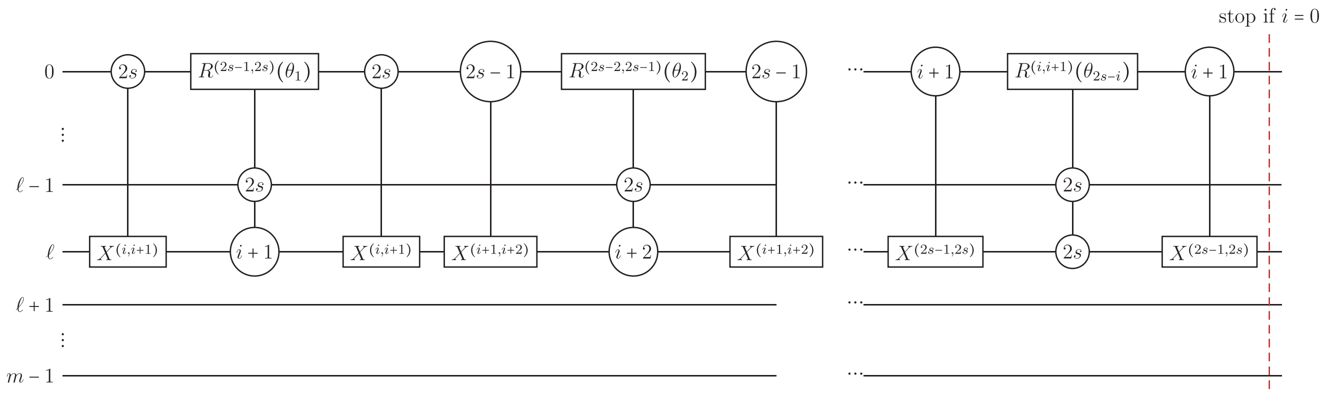

Figure 4. Circuit diagram for $T^{(s)}_{m,k} = T^{(s)}_{m,2s\ell+i} = T^{(s)\,i}_{m;\ell}$ (beginning).

we see that Equation (45) becomes

$$T^{(s)\,i}_{m;\ell}\,|0\rangle^{\otimes(m-\ell-1)}|i\rangle|2s\rangle^{\otimes\ell} = \sum_{j=0}^{i} c^{(s)}_{m,2s\ell+i,j}\,|0\rangle^{\otimes(m-\ell-2)}|i-j\rangle|2s\rangle^{\otimes\ell}|j\rangle$$

$$+\sum_{j=i+1}^{2s} c^{(s)}_{m,2s\ell+i,j}\,|0\rangle^{\otimes(m-\ell-1)}|2s+i-j\rangle|2s\rangle^{\otimes(\ell-1)}|j\rangle \tag{47}$$

Our circuit for $T^{(s)\,i}_{m;\ell}$ generates the terms in Equation (47) from last to first; that is, starting from the reference state on the l.h.s, the circuit successively generates the terms on the r.h.s with $j = 2s, j = 2s-1, \dots, j = 0$. The circuit diagram, split into two parts due to its length, is shown **Figure 4** (beginning) and **Figure 5** (end). If $i = 0$, then the circuit ends at the dashed red line in Figure 4; otherwise, the circuit continues through Figure 5. The $2s$ rotation angles $\theta_1, \dots, \theta_{2s}$ are chosen such that

$$\sin(\theta_1/2)\,\cdots\,\sin(\theta_{2s-j}/2)\,\cos(\theta_{2s+1-j}/2) = c^{(s)}_{m,2s\ell+i,j}\,, j = 0, 1, \dots, 2s \tag{48}$$

where $\theta_{2s+1} \equiv 0$. The displayed circuit diagram is for the generic case with $1 < \ell < m-1$ and $m > 3$; edge cases can be obtained from limits, as for $s = 1/2$ and $s = 1$.

One can easily check that, for $s = 1/2$ and $s = 1$, this circuit reduces to the ones presented in Sections 3 and 4, respectively. Code in cirq[28] for simulating the circuit for $s = 3/2$ is also included in the Supplementary Material.Supporting Information-Supporit

We observe from Figures 4 and 5 that $T^{(s)\,i}_{m;\ell}$ is generically a four-qudit operator (three-qudit for $i = 0$); i.e., the number of qudits on which it acts does not grow with s. Moreover, $T^{(s)\,i}_{m;\ell}$ generically has $2s$ double-controlled rotations, and $4s$ single-controlled NOTs. Recalling that the number of T operators in $U^{(s)}_n$ is $\mathcal{O}(n^2 s)$ Equation (26), we conclude that the total number of gates in $U^{(s)}_n$ is $\mathcal{O}(n^2 s^2)$.

We note that the double-controlled rotation gates can be decomposed into elementary one-qudit and two-qudit gates in the same way as for corresponding double-controlled *qubit* R^y gates, since we use the naive embeddings $SU(2) \subset SU(2s+1)$ Equation (38). Hence, eight two-qudit gates are needed for the decomposition of each double-controlled rotation gate, see e.g. Table 1 in ref. [19]. Universal gate sets for qudit-based quantum computing are reviewed in ref. [30].

5.1. Simplifying the Circuit

As discussed for the cases $s = 1/2$ and $s = 1$ in Sections 3.1 and 4.1 respectively, for a *fixed* value of k, not all T operators are needed; by removing the redundant operators, we are left with a

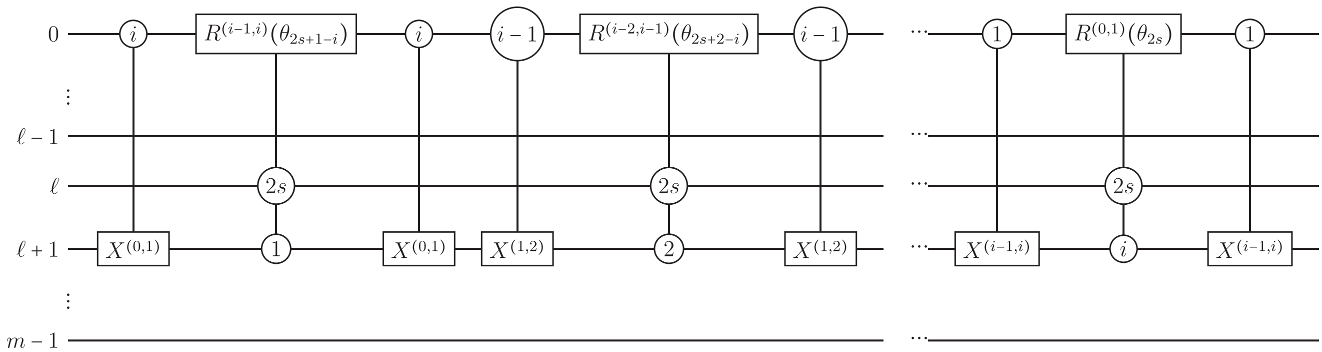

Figure 5. Circuit diagram for $T^{(s)}_{m,k} = T^{(s)}_{m,2s\ell+i} = T^{(s)\,i}_{m;\ell}$ (end). Note that this part of the circuit is present if and only if $i > 0$.

"simplified" k-dependent operator $\mathcal{U}^{(s)}_{n,k}$ that generates the desired state

$$|D^{(s)}_{n,k}\rangle = \mathcal{U}^{(s)}_{n,k}\,|\psi^{(s)}_{n,k}\rangle \tag{49}$$

where

$$\mathcal{U}^{(s)}_{n,k} = \overset{\curvearrowright}{\prod_{m=2}^{n}}\left(\mathcal{W}^{(s)}_{m,k}\otimes \mathbb{I}^{\otimes(n-m)}\right) \tag{50}$$

and

$$\mathcal{W}^{(s)}_{m,k} = \overset{\curvearrowleft}{\prod_{k'=\max(k+2s(m-n),1)}^{\min(k,2sm-1)}} T^{(s)}_{m,k'} \tag{51}$$

see Equations (34) and (44), where again the T operators are given by Figures 4 and 5.

The number of T operators in $\mathcal{U}^{(s)}_{n,k}$ is given, in view of Equations (50) and (51), by

$$\begin{aligned} N^{(s)}_{n,k} &= \sum_{m=2}^{n}\left[1+\min(k,2sm-1)-\max(k+2s(m-n),1)\right] \\ &= \mathcal{O}(k(2sn-k)) \end{aligned} \tag{52}$$

which can be shown to be consistent with the duality symmetry Equation (10)

$$N^{(s)}_{n,k} = N^{(s)}_{n,2sn-k} \tag{53}$$

Hence, the total number of gates in $\mathcal{U}^{(s)}_{n}$ is $\mathcal{O}(sk(2sn-k))$.

6. Discussion

We have introduced the notion of $su(2)$ spin-s Dicke states $|D^{(s)}_{n,k}\rangle$ Equations (5) and (8), which are higher-spin generalizations of usual (spin-1/2) Dicke states that can be decomposed into linear combinations of $su(2s+1)$ qudit Dicke states. Based on the recursive property Equation (17), we have formulated a circuit for preparing these states. (Specifically, we have determined a k-independent operator $U^{(s)}_{n}$ that generates via Equation (11) these spin-s Dicke states from reference states $|\psi^{(s)}_{n,k}\rangle$ in terms of W's Equation (21), which are in turn given in terms of T's Equation (25); and the T's are (at most) four-qudit operators given by the circuits in Figures 4 and 5.) These Dicke states can also be generated with a "simplified" k-dependent operator $\mathcal{U}^{(s)}_{n,k}$ using fewer T operators, see Equations (49)–(51). We emphasize that this algorithm for preparing Dicke states $|D^{(s)}_{n,k}\rangle$ is deterministic, does not use ancillary qudits, and the number of gates scales as $sk(2sn-k)$, see Equation (52); this circuit is therefore efficient[1] to the extent that its size is polynomial in the system size n (as well as the spin s and the parameter k). These circuits are significantly simpler than those for preparing $(2s+1)$-level qudit Dicke states.[19]

We have also precisely related spin-s Dicke states to $(2s+1)$-level qudit Dicke states Equations (A10) and (A13), and we have computed their entanglement entropy Equations (C3) and (C6). Because spin-s Dicke states are linear combinations of qudit Dicke states, one could use quantum phase estimation to project a spin-s Dicke state onto a desired qudit Dicke state, with success probability $|\alpha^{(s)}_{n,k}(\vec{k})|^2$ (A13), see refs. [31, 32].

Further properties and applications of spin-s Dicke states remain to be explored. For example, it would be interesting to consider their q-deformation, and compare with corresponding results for $(2s+1)$-level qudit Dicke states. Indeed, it was shown[21] that celebrated q-combinatorial identities arise naturally from the q-analog qudit Dicke states; perhaps other identities can be related to the q-analog of the spin-s Dicke states, such as (possibly) a q-analog of Equation (A14). Moreover, as noted in the Introduction, these states may be useful for generalizing the many applications of (qubit) Dicke states to qudits, and may serve as the starting point for preparing exact eigenstates of integrable higher-spin Heisenberg chains.

Appendix A: Spin-s Dicke States in Terms of $(2s+1)$-Level Qudit Dicke States

We derive here the closed-form Equation (8) for the spin- s Dicke states by expressing the $su(2)$ spin-s Dicke states in terms of $su(2s+1)$ qudit Dicke states, see Equation (A10) below.

A.1. Qudit Dicke States

We begin by defining a multiset $M(\vec{k})$

$$M(\vec{k}) = \{\underbrace{0,\ldots,0}_{k_0},\underbrace{1,\ldots,1}_{k_1},\ldots,\underbrace{d-1,\ldots,d-1}_{k_{d-1}}\} \tag{A1}$$

where k_j is the multiplicity of j in $M(\vec{k})$, such that $M(\vec{k})$ has cardinality n. Hence, $\vec{k}$ is a d-dimensional vector such that

$$\vec{k} = (k_0,k_1,\ldots,k_{d-1}) \quad \text{with} \quad k_j\in\{0,1,\ldots,n\} \quad \text{and} \quad \sum_{j=0}^{d-1}k_j = n \tag{A2}$$

The corresponding normalized qudit Dicke state $|D^n(\vec{k})\rangle$ with a number n of d-level qudits is defined by (see[19] and references therein)

$$|D^n(\vec{k})\rangle = \frac{1}{\sqrt{\binom{n}{\vec{k}}}}\sum_{w\in\mathfrak{S}_{M(\vec{k})}}|w\rangle \tag{A3}$$

where $\mathfrak{S}_{M(\vec{k})}$ is the set of permutations of the multiset $M(\vec{k})$ (A1), and $|w\rangle$ is the n-qudit state corresponding to the permutation w. Moreover, $\binom{n}{\vec{k}}$ denotes the multinomial

$$\binom{n}{\vec{k}} = \binom{n}{k_0,k_1,\ldots,k_{d-1}} = \frac{n!}{\prod_{j=0}^{d-1}k_j!} \tag{A4}$$

The qudit Dicke states satisfy the recursion[19]

$$|D^n(\vec{k})\rangle = \sum_{j=0}^{d-1}\sqrt{\frac{k_j}{n}}\,|D^{n-1}(\vec{k}-\hat{j})\rangle\otimes|j\rangle \tag{A5}$$

where $\hat{j}$ is the d-dimensional unit vector with components $(\hat{j})_a=\delta_{aj}$, $a=0,1,\ldots,d-1$.

A.2. Higher-Spin Dicke States in Terms of Qudit Dicke States

As a simple example of a spin-s Dicke state in terms of $(2s+1)$-level qudit Dicke states, we observe that the spin-1 Dicke state Equation (9) can be rewritten as

$$|D^{(1)}_{3,2}\rangle = \frac{2}{\sqrt{5}}|D^3(1,2,0)\rangle + \frac{1}{\sqrt{5}}|D^3(2,0,1)\rangle \tag{A6}$$

We now proceed to generalize this result.

Because the spin-s Dicke state $|D^{(s)}_{n,k}\rangle$ is invariant under any permutation, we know it can be decomposed into a linear combination of the permutation-invariant d-level qudit Dicke states $|D^n(\vec{k})\rangle$, as in Equation (A6). Evidently, we need $d = 2s+1$. Moreover, we observe that such a qudit Dicke state is an eigenstate of $\mathbb{S}^z$ with eigenvalue $sn - \sum_{j=0}^{2s} j\, k_j$; and since the $\mathbb{S}^z$ eigenvalue of the spin-s Dicke state $|D^{(s)}_{n,k}\rangle$ is given by $sn-k$, the decomposition is restricted to $\vec{k}$'s that satisfy

$$\sum_{j=0}^{2s} j\, k_j = k \tag{A7}$$

We also require that the number of qudits match, so

$$\sum_{j=0}^{2s} k_j = n \tag{A8}$$

see Equation (A2). In other words, for given values of n, k and s, the allowed values of $\vec{k} = (k_0, k_1, \ldots, k_{2s})$ are precisely the solutions of the Diophantine Equations (A7) and (A8). The number of such solutions, which we denote by $g^{(s)}_{n,k}$, is known to be generated by the q-binomial coefficient[33, 35]

$$\binom{n+2s}{2s}_q = \sum_{k=0}^{2sn} g^{(s)}_{n,k}\, q^k \tag{A9}$$

We conclude that a spin-s Dicke state has the decomposition

$$\left|D^{(s)}_{n,k}\right\rangle = \sum_{\vec{k}}{}' \alpha^{(s)}_{n,k}(\vec{k})\, |D^n(\vec{k})\rangle \tag{A10}$$

where the sum over $\vec{k}$ is restricted (indicated by a prime) to solutions of Equations (A7) and (A8), and the coefficients $\alpha^{(s)}_{n,k}(\vec{k})$ are still to be determined.

In order to determine the coefficients $\alpha^{(s)}_{n,k}(\vec{k})$, we substitute Equation (A10) into the recursion Equation (17), and obtain

$$\sum_{\vec{k}}{}' \alpha^{(s)}_{n,k}(\vec{k})\, |D^n(\vec{k})\rangle = \sum_{j=0}^{2s} c^{(s)}_{n,k,j} \sum_{\vec{a}}{}'' \alpha^{(s)}_{n-1,k-j}(\vec{a})\, |D^{n-1}(\vec{a})\rangle \otimes |j\rangle \tag{A11}$$

where on the r.h.s we restrict (indicated by a double-prime) $\vec{a}$ to be solutions of Equations (A7) and (A8) with $k_j \to a_j$, $n \to n-1$, $k \to k-j$. Expanding $|D^n(\vec{k})\rangle$ in Equation (A11) via the qudit Dicke state recursion Equation (A5), and making the association $\vec{a} \to \vec{k} - \hat{j}$ then gives a recursive relation for the coefficients $\alpha^{(s)}_{n,k}(\vec{k})$

$$\sqrt{\frac{k_j}{n}}\, \alpha^{(s)}_{n,k}(\vec{k}) = c^{(s)}_{n,k,j}\, \alpha^{(s)}_{n-1,k-j}(\vec{k}-\hat{j}) \tag{A12}$$

which solves to

$$\alpha^{(s)}_{n,k}(\vec{k}) = \left[\frac{\binom{n}{\vec{k}}}{\binom{2sn}{k}} \prod_{j=0}^{2s} \binom{2s}{j}^{k_j} \right]^{1/2} \tag{A13}$$

We note that the orthonormality of the spin-s and qudit Dicke states thus implies the combinatorial identity[34]

$$\binom{2sn}{k} = \sum_{\vec{k}} \binom{n}{\vec{k}} \prod_{j=0}^{2s} \binom{2s}{j}^{k_j}, \tag{A14}$$

where we sum over solutions $\vec{k}$ to the Diophantine Equations (A7) and (A8). Finally, Equation (8) follows from Equations (A3), (A10), and (A13).

The paper[27] includes a discussion of particular cases of the results Equations (A10) and (A13). Specifically, for the three cases $s = 1, 3/2, 2$, formulas for the coefficients $\alpha^{(s)}_{n,k}(\vec{k})$ are given in ref. [27] (note that our variables $(n, k, \vec{k})$ correspond to the variables $(N, J-M, \vec{n})$ in ref. [27], with $J = sN$), see there Equations (14), (28), and (44); and sample values of these coefficients are reported in corresponding tables. Where there is overlap, our results agree with those in ref. [27], apart from some typos in the latter.

A.3. An Alternative Construction of Spin-s Dicke States

Since a spin-s Dicke state can be expressed Equation (A10) as a linear combination of $(2s+1)$-level qudit Dicke states, the construction[19] of the latter can—in principle—be used to obtain an alternative construction of the former. Indeed, a unitary operator U_n is found in ref. [19] that generates the qudit Dicke state Equation (A3) from a product state $|\mathrm{e}(\vec{k})\rangle$

$$U_n\, |\mathrm{e}(\vec{k})\rangle = |D^n(\vec{k})\rangle, \qquad |\mathrm{e}(\vec{k})\rangle = |0\rangle^{\otimes k_0} |1\rangle^{\otimes k_1} \ldots |d-1\rangle^{\otimes k_{d-1}} \tag{A15}$$

It is not difficult to prepare the linear combination of the $|\mathrm{e}(\vec{k})\rangle$'s

$$|\alpha^{(s)}_{n,k}(\vec{k})\rangle = \sum_{\vec{k}}{}' \alpha^{(s)}_{n,k}(\vec{k})\, |\mathrm{e}(\vec{k})\rangle \tag{A16}$$

where the coefficients $\alpha^{(s)}_{n,k}(\vec{k})$ are given by Equation (A13). It follows from Equations (A10), (A15), and (A16) that the spin-s Dicke state can be constructed by acting with U_n on the above state

$$|D^{(s)}_{n,k}\rangle = U_n\, |\alpha^{(s)}_{n,k}(\vec{k})\rangle \tag{A17}$$

(This is similar to the construction of a linear combination of qubit Dicke states in Theorem 2 of ref. [11].) However, the quantum circuit for U_n in ref. [19] is considerably more complicated than the circuit for $U^{(s)}_n$ Equation (11) in the present work.

Appendix B: Proof of the Recursion Equation (17)

In this section, we denote the total spin operators Equation (3) by $\vec{\mathbb{S}}^{(n)}$ in order to indicate the number of spins (qudits). It follows from Equation (3) that these operators satisfy the recursion

$$\vec{\mathbb{S}}^{(n)} = \vec{\mathbb{S}}^{(n-1)} \otimes \mathbb{I} + \mathbb{I}^{\otimes(n-1)} \otimes \vec{S} \tag{B1}$$

where $\vec{S} = \vec{\mathbb{S}}^{(1)}$. Therefore, powers of the total spin-lowering operator are given by

$$\left(\mathbb{S}^{(n)-}\right)^k = \left(\mathbb{S}^{(n-1)-} \otimes \mathbb{I} + \mathbb{I}^{\otimes(n-1)} \otimes S^-\right)^k = \sum_{j=0}^{k} \binom{k}{j} \left(\mathbb{S}^{(n-1)-}\right)^{k-j} \otimes (S^-)^j \tag{B2}$$

Recalling the definition Equation (5) of spin-s Dicke states, we obtain

$$\begin{aligned} |D^{(s)}_{n,k}\rangle &= a^{(s)}_{n,k} \left(\mathbb{S}^{(n)-}\right)^k |0\rangle^{\otimes n} \\ &= a^{(s)}_{n,k} \left\{ \sum_{j=\max(0,k-2s(n-1))}^{\min(k,2s)} \binom{k}{j} \left(\mathbb{S}^{(n-1)-}\right)^{k-j} \otimes (S^-)^j \right\} \left(|0\rangle^{\otimes(n-1)} \otimes |0\rangle\right) \end{aligned} \tag{B3}$$

where the limits in the sum reflects the fact that $\left(\mathbb{S}^{(n)-}\right)^j |0\rangle^{\otimes n} = 0$ for $j > 2sn$. Noting also that

$$a^{(s)}_{1,j} (S^-)^j |0\rangle = |j\rangle, \qquad j = 0, 1, \dots, 2s \tag{B4}$$

we conclude from Equation (B3) that

$$|D^{(s)}_{n,k}\rangle = \sum_{j=\max(0,k-2s(n-1))}^{\min(k,2s)} c^{(s)}_{n,k,j} \, |D^{(s)}_{n-1,k-j}\rangle \otimes |j\rangle \tag{B5}$$

where

$$c^{(s)}_{n,k,j} = \binom{k}{j} \frac{a^{(s)}_{n,k}}{a^{(s)}_{n-1,k-j}\, a^{(s)}_{1,j}} = \sqrt{\frac{\binom{2s}{j}\binom{2sn-2s}{k-j}}{\binom{2sn}{k}}} \tag{B6}$$

where we used the result Equation (7) to pass to the the final equality. Focusing on the limits in the sum in Equation (B5), and recalling the definition of ℓ Equation (12), we note that $k < 2s$ implies $\ell = 0$, and $k - 2s(n-1) > 0$ implies $\ell = n - 1$ (or the trivial case $\ell = n$). Because the circuits for $\ell = 0, 1, n-1$ will be treated separately as edge cases of the circuit for $1 < \ell < n - 1$, instead of Equation (B5) we simply write

$$|D^{(s)}_{n,k}\rangle = \sum_{j=0}^{2s} c^{(s)}_{n,k,j} \, |D^{(s)}_{n-1,k-j}\rangle \otimes |j\rangle \tag{B7}$$

assuming $1 < \ell < n - 1$.

Appendix C: Entanglement Entropy

Usual (spin-1/2) Dicke states have long been known to be entangled; indeed, the simplest such state $|D_{2,1}\rangle = (|01\rangle + |10\rangle)/\sqrt{2}$ is a Bell state. The Von Neumann bipartite entanglement entropy of a Dicke state $|D_{n,k}\rangle$ for general values of n and k was computed in refs. [36, 37], see also refs. [38–40]. Corresponding results were obtained for qudit Dicke states $|D^n(\vec{k})\rangle$ (A3) in refs. [41, 42], as well as for their q-analogs in refs. [20, 21].

We calculate here the bipartite entanglement entropy of the spin-s Dicke states $|D^{(s)}_{n,k}\rangle$ Equation (5). This entails partitioning the n qudits into two parts, of sizes $n - l$ and l, where $l < n$ is a positive integer, and calculating the eigenvalues of the reduced density matrix of $|D^{(s)}_{n,k}\rangle$, obtained by tracing over the first $n - l$ qudits of the density matrix. One method of computing these eigenvalues is to find the Schmidt decomposition for the spin-s Dicke states, which we claim is given by

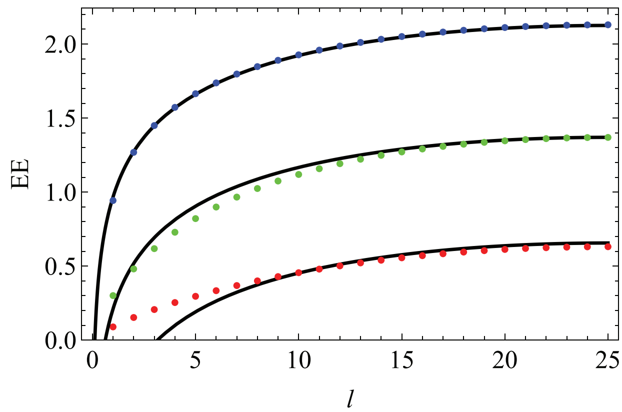

Figure C1. The entanglement entropy (EE) of the state $|D^{(s)}_{n,k}\rangle$ as a function of l for $s = 1$, $n = 50$. The exact values are given for $k = 1$ (red), $k = 5$ (green), and $k = 50$ (blue), as are their respective approximated curves (black).

$$|D^{(s)}_{n,k}\rangle = \sum_{j=\max(0,k-2s(n-l))}^{\min(k,2sl)} \sqrt{\lambda_j}\, |D^{(s)}_{n-l,k-j}\rangle \otimes |D^{(s)}_{l,j}\rangle \tag{C1}$$

where

$$\lambda_j = \frac{\binom{2sl}{j}\binom{2sn-2sl}{k-j}}{\binom{2sn}{k}} \tag{C2}$$

Note that the max/min in Equation (C1) are simply enforcing the requirements $0 \le j \le 2sl$ and $0 \le k - j \le 2sn - 2sl$. A proof for this decomposition can be obtained by generalizing the argument in Appendix B; indeed, the recursion Equation (B5) can be viewed as a special case of the Schmidt decomposition Equation (C1) with $l = 1$, as we see that $\sqrt{\lambda_j} = c^{(s)}_{n,k,j}$ when $l = 1$. Using the orthonormality of the spin-s Dicke states, it follows from the Schmidt decomposition that the eigenvalues of the reduced density matrix are given by λ_j, and therefore the entanglement entropy of $|D^{(s)}_{n,k}\rangle$ is given by

$$S_l = \sum_{j=\max(0,k-2s(n-l))}^{\min(k,2sl)} -\lambda_j \log_{2s+1} \lambda_j \tag{C3}$$

We observe that λ_j, and therefore S_l, are invariant under $k \to 2sn - k$, corresponding to the duality symmetry Equation (10). This allows us to focus on the case $k \le sn$. Note that while $\lambda_j \equiv \lambda_j(l)$ is not symmetric under $l \to n - l$, it does satisfy $\lambda_j(l) = \lambda_{k-j}(n-l)$. It follows that S_l is also symmetric under $l \to n - l$, so we restrict our attention to $l \le n/2$. Following,[37] for large n and l, we can approximate the hypergeometric distribution λ_j via the Gaussian distribution

$$\lambda_j \approx \frac{1}{\sqrt{2\pi}\sigma} \exp\left[-\frac{(j-\bar{j})^2}{2\sigma^2}\right] \tag{C4}$$

with mean $\bar{j} = kl/n$ and variance

$$\sigma^2 = k(2sn-k)l(n-l)/2sn^3 \tag{C5}$$

the latter of which exhibits the expected symmetries $l \to n - l$ and $k \to 2sn - k$. The entanglement entropy is therefore approximated by

$$S_l \approx -\int_{-\infty}^{\infty} \lambda_j \log_{2s+1} \lambda_j \, dj = \frac{1}{2} \log_{2s+1}(2\pi e \sigma^2) \tag{C6}$$

We plot the entanglement entropy curves—both the numerical sums given by Equation (C3) and the approximated curves given by Equation (C6)—for $s = 1$ in **Figure C1**. The results are qualitatively similar to those for the case $s = 1/2$.[36,37] Indeed, the variance Equation (C5) for fixed n, k, s, l can be mapped to the variance for the usual (spin-1/2) Dicke state $|D_{2sn,k}\rangle$ with partitions of sizes $2sl$ and $2sn - 2sl$. In other words, denoting the result in Equation (C5) by $\sigma^2(n, k, s, l)$, we see that

$$\sigma^2(n, k, s, l) = \sigma^2(2sn, k, \frac{1}{2}, 2sl) \tag{C7}$$

corresponding to the mapping $(n, l) \mapsto (2sn, 2sl)$, i.e. "stretching" both the chain and the partition by the factor $2s$.

Comparing the entanglement entropy results for spin-s Dicke states and for $(2s+1)$-level qudit Dicke states,[41,42] we find that they cannot be mapped into each other (such as in Equation (C7)) except for $s = 1/2$. This is not surprising, given that the latter states have $2s + 1$ free parameters ($\vec{k}$, where $n = \sum_i k_i$), while the former states have only two (n and k).

Appendix D:

Circuit Diagrams for $s = 1$ Edge Cases

For completeness, we display here circuit diagrams corresponding to the various edge cases for $s = 1$ (**Figure D1–D5**).

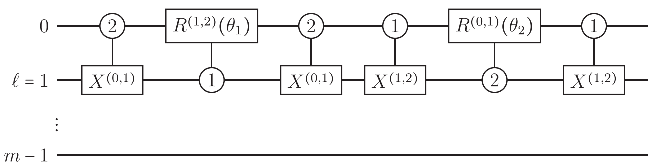

Figure D1. Circuit diagram for $T^{(1)}_{m,k} = T^{(1)}_{m,2\ell} = T^{(1)\,0}_{m;\ell}$ (k even), with $\ell = 1$, $m > 1$.

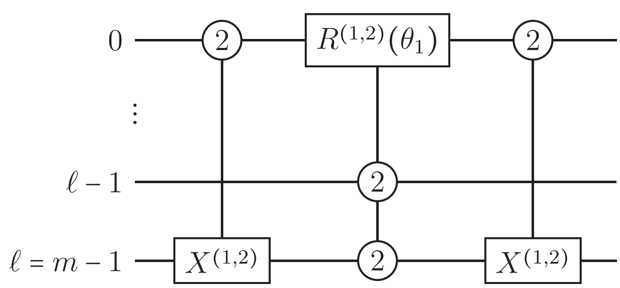

Figure D2. Circuit diagram for $T^{(1)}_{m,k} = T^{(1)}_{m,2\ell+1} = T^{(1)\,1}_{m;\ell}$ (k odd), with $\ell = m - 1$, $m > 2$.

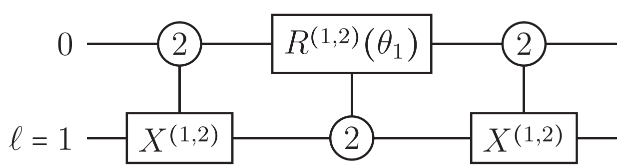

Figure D3. Circuit diagram for $T^{(1)}_{m,k} = T^{(1)}_{m,2\ell+1} = T^{(1)\,1}_{m;\ell}$ (k odd), with $\ell = 1$, $m = 2$.

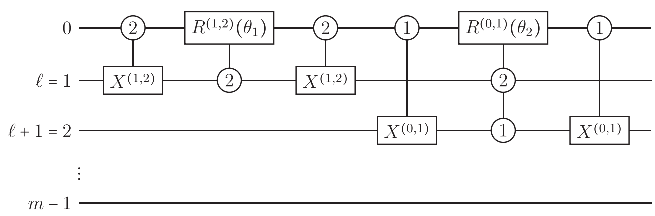

Figure D4. Circuit diagram for $T^{(1)}_{m,k} = T^{(1)}_{m,2\ell+1} = T^{(1)\,1}_{m;\ell}$ (k odd), with $\ell = 1$, $m > 2$.

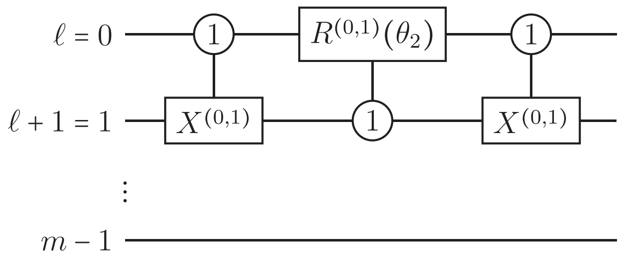

Figure D5. Circuit diagram for $T^{(1)}_{m,k} = T^{(1)}_{m,2\ell+1} = T^{(1)\,1}_{m;\ell}$ (k odd), with $\ell = 0$, $m > 1$.

Acknowledgements

The authors thank Matthias Christandl for discussions. R.N. acknowledges the hospitality and financial support from INFN BO and Bologna University (ISA Visiting Fellowship), where this work was initiated. R.N. was also supported in part by the National Science Foundation under grant PHY 2310594, and by a Cooper fellowship. F.R. thanks the RFO funds of the Department of Physics and Astronomy of Bologna University and INFN for financial support through the GAST and DOT4 grants.

Conflict of Interest

The authors declare no conflict of interest.

Data Availability Statement

The data that support the findings of this study are available in the supplementary material Supporting Information for of this article.

Keywords

Dicke states, entanglement entropy, quantum state preparation, qudits

Received: February 11, 2024
Revised: July 30, 2024
Published online:

[1] M. A. Nielsen, I. L. Chuang, *Quantum Computation and Quantum Information*, Cambridge University Press, Cambridge **2019**.
[2] A. Barenco, C. H. Bennett, R. Cleve, D. P. Divincenzo, N. Margolus, P. Shor, T. Sleator, J. A. Smolin, H. Weinfurter, *Phys. Rev. A* **1995**, *52*, 3457.
[3] P. Kaye, M. Mosca, *Optical Fiber Communication Conference and International Conference on Quantum Information ICQI*, **2004**.

[4] M. Mottonen, J. J. Vartiainen, V. Bergholm, M. M. Salomaa, *Quant. Inf. Comp.* **2005**, *5*, 467.
[5] V. V. Shende, S. S. Bullock, I. L. Markov, *IEEE Trans on Computer-Aided Design* **2006**, *25*, 1000.
[6] M. Plesch, Č. Brukner, *Phys. Rev. A* **2011**, *83*, 032302.
[7] R. H. Dicke, *Phys. Rev.* **1954**, *93*, 99.
[8] R. Prevedel, G. Cronenberg, M. S. Tame, M. Paternostro, P. Walther, M. S. Kim, A. Zeilinger, *Phys. Rev. Lett.* **2009**, *103*, 020503.
[9] G. Tóth, *Phys. Rev. A* **2012**, *85*, 022322.
[10] E. Farhi, J. Goldstone, S. Gutmann, *arXiv:1411.4028* **2014**.
[11] A. Bärtschi, S. Eidenbenz, *Lecture Notes in Computer Science* **2019**, 126.
[12] K. Chakraborty, B.-S. Choi, A. Maitra, S. Maitra, *Quant. Inf. Comp.* **2014**, *13*, 2049.
[13] A. Bärtschi, S. Eidenbenz, *2022 IEEE Int. Conf. Quant. Comp. Eng.*, **2022**, 87.
[14] J. S. Van Dyke, G. S. Barron, N. J. Mayhall, E. Barnes, S. E. Economou, *PRX Quantum* **2021**, *2*, 040329.
[15] J. S. Van Dyke, E. Barnes, S. E. Economou, R. I. Nepomechie, *J. Phys. A* **2022**, *55*, 055301.
[16] W. Li, M. Okyay, R. I. Nepomechie, *J. Phys. A* **2022**, *55*, 355305.
[17] H. Bethe, *Z. Phys.* **1931**, *71*, 205.
[18] M. Gaudin, *La fonction d'onde de Bethe*. Masson, 1983. English translation by J.-S. Caux, *The Bethe wavefunction*, Cambridge University Press, Cambridge **2014**.
[19] R. I. Nepomechie, D. Raveh, *Quantum Inf. Comp.* **2024**, *24*, 0037.
[20] Z.-H. Li, A.-M. Wang, *Int. J. Quant. Inf.* **2015**, *13*, 1550007.
[21] D. Raveh, R. I. Nepomechie, *J. Phys. A* **2024**, *57*, 065302.
[22] F. Mozafari, G. De Micheli, Y. Yang, *Phys. Rev. A* **2022**, *106*, 022617.
[23] L. Yeh, *Proceedings of QP2023*, ACM, New York **2023**.
[24] N. Crampé, E. Ragoucy, L. Alonzi, *SIGMA* **2011**, *7*, 006.
[25] H. J. Lipkin, N. Meshkov, A. J. Glick, *Nucl. Phys.* **1965**, *62*, 188.
[26] After this work was completed, we became aware of ref. [27], which has some overlap with Appendix A. We thank a referee for bringing this reference to our attention.
[27] W.-F. Liu, Z.-D. Hu, *arXiv:1511.0328* **2015**.
[28] Quantum AI team and collaborators, qsim, **2020**, https://doi.org/10.5281/zenodo.4023103 (accessed: August 2024).
[29] Y.-M. Di, H.-R. Wei, *Phys. Rev. A* **2013**, *87*, 012325.
[30] Y. Wang, Z. Hu, B. C. Sanders, S. Kais, *Front. Phys.* **2020**, *8*, 479.
[31] Y. Wang, B. M. Terhal, *Phys. Rev. A* **2021**, *104*.
[32] L. Piroli, G. Styliaris, J. I. Cirac, *arXiv:2403.07604* **2024**.
[33] Indeed, in the language of ref. [35] on page 65, the multiset $M(\vec{k})$ Equation (A1) with $d = 2s + 1$ defines a *partition* of k (defined in Equation (A7)), and the nonzero elements of $M(\vec{k})$ are its *parts*; according to Proposition 1.7.3 in ref. [35], the number of partitions of k into at most n parts, with largest part at most $2s$, is given by $g^{(s)}_{n,k}$ in Equation (A9). We thank Michelle Wachs for pointing us to this reference.
[34] This identity follows from Faà di Bruno's formula when considering k derivatives of $f(g(x))$ with $f(x) = x^n$ and $g(x) = (1 + x)^{2s}$ and evaluating at $x = 0$. We thank Math Stack Exchange user 'ameg' for pointing out to us this proof.
[35] R. P. Stanley, *Enumerative Combinatorics*, 2nd ed., Vol. *1*, Cambridge University Press, Cambridge **2011**.
[36] V. Popkov, M. Salerno, *Phys. Rev. A* **2005**, *71*, 012301.
[37] J. I. Latorre, R. Orus, E. Rico, J. Vidal, *Phys. Rev. A* **2005**, *71*, 064101.
[38] B. Lücke, J. Peise, G. Vitagliano, J. Arlt, L. Santos, G. Tóth, C. Klempt, *Phys. Rev. Lett.* **2014**, *112*, 155304.
[39] M. G. M. Moreno, F. Parisio, *arXiv:1801.00762* **2018**.
[40] W. Munizzi, H. J. Schnitzer, *Phys. Rev. A* **2024**, *109*, 012405.
[41] V. Popkov, M. Salerno, G. Schütz, *Phys. Rev. A* **2005**, *72*, 032327.
[42] J. A. Carrasco, F. Finkel, A. González-López, M. A. Rodríguez, P. Tempesta, *J. Stat. Mech.* **2016**, *1603*, 033114.

